

Bit-Efficient Quantisation for Two-Channel Modulo-Sampling Systems

Wenyi Yan, Zeyuan Li, Lu Gan, Honqing Liu, Guoquan Li

Abstract—Two-channel modulo analog-to-digital converters (ADCs) enable high-dynamic-range signal sensing at the Nyquist rate per channel, but existing designs quantise both channel outputs independently, incurring redundant bitrate costs. This paper proposes a bit-efficient quantisation scheme that exploits the integer-valued structure of inter-channel differences, transmitting one quantised channel output together with a compact difference index. We prove that this approach requires only 1–2 bits per signal sample overhead relative to conventional ADCs, despite operating with a much smaller per-channel dynamic range. Simulations confirm the theoretical error bounds and bitrate analysis, while hardware experiments demonstrate substantial bitrate savings compared with existing modulo sampling schemes, while maintaining comparable reconstruction accuracy. These results highlight a practical path towards high-resolution, bandwidth-efficient modulo ADCs for bitrate-constrained systems.

Index Terms—Unlimited sensing framework, Multi-channel systems, High dynamic range signals, Quantisation, Bitrate efficiency, Chinese remainder theorem.

I. INTRODUCTION

The unlimited sensing framework (USF) prevents clipping by folding high-amplitude signals into a low dynamic range, enabling digital recovery of signals that would otherwise saturate [1]–[11]. Several hardware prototypes have further demonstrated the potential of single-channel USF systems in practice [2], [12]–[15]. Although a variety of algorithms and hardware implementations exist, single-channel USF systems typically require high oversampling rates and complex reconstruction procedures, limiting their suitability for bitrate-constrained or low-cost receivers.

Multi-channel architectures [16]–[20] based on the robust Chinese Remainder Theorem (RCRT) [21]–[23] offer a compelling alternative. By employing channels with distinct dynamic ranges, they achieve high overall range without per-channel oversampling [17], [18], [21]. Beyond RCRT, Guo *et al.* [24] proved perfect recovery for finite-rate-of-innovation (FRI) signals under irrational threshold ratios in two-channel modulo sampling systems. However, such a ratio is impractical in hardware and its recovery relies on exhaustive search over wrapping indices. Several recent works have studied sub-Nyquist architectures for complex sinusoidal mixtures [10], [25], [26] by employing multicoset sampling with amplitude-unfolding and spectral estimation. Besides, Wang *et al.* [27] formulate sinusoidal estimation as a mixed-integer program using first-order differences and a multi-channel “virtual”

This work has been submitted to the IEEE for possible publication. Copyright may be transferred without notice, after which this version may no longer be accessible.

modulo ADC to enlarge the effective dynamic range. Florescu [28] proposes a multi-channel architecture with a shared folding loop to improve noise robustness via averaging.

A key challenge in multi-channel modulo-ADC systems is quantisation efficiency. In existing designs, each channel is sampled and quantised independently using b bits per modulo sample. In particular, [18] and [26] provide closed-form expressions for the minimum required b in systems with L real-valued moduli and two complex-valued moduli, respectively. The total bitrates can be much higher than those of a conventional ADC. To overcome this limitation, we develop an Efficient CRT (ECRT) quantisation scheme that exploits inter-channel redundancy within a two-channel modulo sampling architecture. Our main contributions are as follows:

- **Bit-efficient quantisation:** The proposed ECRT transmits the quantised modulo samples from *one* channel together with a compact quantised inter-channel difference, eliminating redundancy and substantially reducing the total bits per signal sample compared with existing two-channel systems [18].
- **Theoretical guarantees:** Closed-form bounds on the recovery error and bit requirements are derived, showing that ECRT requires only a 1–2 bit per sample overhead relative to a conventional high-dynamic-range ADC, with a single-bit overhead in most cases.
- **Simulation and hardware validation:** Simulations confirm the theoretical error bounds and bitrate predictions, while hardware experiments demonstrate that ECRT achieves a significantly lower bitrate than single-channel modulo sampling schemes, offering a more communication-efficient solution.

II. BACKGROUND AND MOTIVATION

For an input $x \in \mathbb{R}$ and ADC dynamic range $\Delta > 0$, the modulo operation is defined as [3]

$$\langle x \rangle_{\Delta} = x - \Delta \left\lfloor \frac{x}{\Delta} + \frac{1}{2} \right\rfloor, \quad (1)$$

which folds x into $[-\frac{\Delta}{2}, \frac{\Delta}{2})$. Consider a bandlimited signal $g(t)$ processed by a two-channel modulo-ADC system with

$$\Delta_{\ell} = \tau_{\ell} \varepsilon, \quad \ell = 1, 2, \quad (2)$$

where τ_1, τ_2 are coprime integers satisfying $2 \leq \tau_1 < \tau_2$, and $\varepsilon > 0$ is a scaling factor. Sampling at period T yields

$$\tilde{y}_{\ell}[k] = \langle g(kT) \rangle_{\Delta_{\ell}} + e_{\ell}[k] = y_{\ell}[k] + e_{\ell}[k], \quad k \in \mathbb{Z}, \quad (3)$$

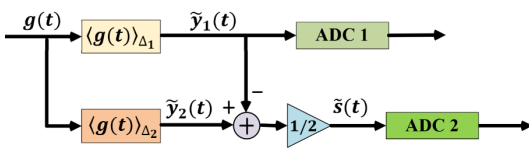


Fig. 1. Proposed bit-efficient two-channel modulo-ADC architecture. Channel 1 quantises $y_1(t)$, while Channel 2 quantises the scaled signal $\tilde{s}(t)$.

where $y_\ell[k] = \langle g[k] \rangle_{\Delta_\ell}$ is the noiseless modulo output and $e_\ell[k]$ is the folding noise. $g[k]$ can be written as

$$g[k] = \Delta_\ell n_\ell[k] + y_\ell[k], \quad (4)$$

where $n_\ell[k] \in \mathbb{Z}$ are folding indices. Quantising each $\tilde{y}_\ell[k]$ with b bits gives

$$\hat{y}_\ell[k] = \tilde{y}_\ell[k] + q_\ell[k] = y_\ell[k] + e_\ell[k] + q_\ell[k], \quad k \in \mathbb{Z}, \quad (5)$$

in which the quantisation noise $q_\ell[k]$ is bounded by $|q_\ell[k]| \leq \Delta_\ell/2^{b+1}$. RCRT estimates folding indices from $\hat{y}_1[k] - \hat{y}_2[k]$ and reconstructs via [21]

$$\hat{g}_{\text{RCRT}}[k] = \frac{1}{2} \left(\hat{n}_1[k] \Delta_1 + \hat{y}_1[k] + \hat{n}_2[k] \Delta_2 + \hat{y}_2[k] \right). \quad (6)$$

Stable recovery ($\hat{n}_\ell[k] = n_\ell[k]$) is guaranteed when [21]

$$|e_2[k] - e_1[k]| + \frac{\Delta_1 + \Delta_2}{2^{b+1}} < \frac{\varepsilon}{2} \quad (7)$$

The bit-depth requirement for stable recovery is [18]

$$B_{\text{RCRT}} = 2b, \quad \text{with } b \geq \lceil \log_2(\tau_1 + \tau_2) \rceil, \quad (8)$$

where B_{RCRT} is the total number of bits per sample, and equality holds when folding noise is absent ($e_\ell[k] = 0$).

For comparison, define the amplitude scaling factor

$$\rho = 2\|g(t)\|_\infty / \Delta, \quad (9)$$

and let B_c denote the bit cost of a conventional ADC (same quantisation step). Then [18]

$$B_c = b + \lceil \log_2 \rho \rceil. \quad (10)$$

For a given ρ , we need $\tau_1 \geq \rho$ and $\tau_2 \geq \rho + 1$ [18], yielding $b \geq \lceil \log_2(\rho + 1) + 1 \rceil$ and an overhead

$$B_{\text{RCRT}} - B_c = b - \lceil \log_2 \rho \rceil, \quad (11)$$

that grows linearly with b . We next introduce a quantisation scheme reducing this overhead to only 1 to 2 bits.

III. PROPOSED BIT-EFFICIENT TWO-CHANNEL DESIGN

A. System Model

To obtain a bit-efficient scheme, we first exploit the inter-channel redundancy. Define the normalised difference $d[k] = \frac{y_2[k] - y_1[k]}{\varepsilon}$. From (2) and (4),

$$d[k] = \frac{y_2[k] - y_1[k]}{\varepsilon} = \tau_1 n_1[k] - \tau_2 n_2[k],$$

so $d[k] \in \mathbb{Z}$. Using $-\Delta_\ell/2 \leq y_\ell[k] < \Delta_\ell/2$, we obtain $|d[k]| < (\tau_1 + \tau_2)/2$, showing that $d[k]$ takes at most $\tau_1 + \tau_2$ integer values. However, directly forming the difference

$y_2[k] - y_1[k]$ expands the dynamic range to $(\Delta_1 + \Delta_2)$, which exceeds the range of either ADC. To avoid this saturation issue, we instead sample the scaled difference $s[k] = \frac{y_2[k] - y_1[k]}{2}$, for which $|s[k]| < (\Delta_1 + \Delta_2)/2 < \Delta_2/2$. Thus $s[k]$ always lies strictly within the dynamic range of the second ADC.

These observations motivate the proposed two-channel modulo sampling architecture in Fig. 1 and the associated quantisation and recovery scheme in Alg. 1. Theorem 1 quantifies the bit budget required by the proposed design and establishes its stability under bounded noise.

Theorem 1 (ECRT: quantisation and stable recovery). *Consider the two-channel modulo sampling system in Fig. 1 with dynamic ranges $\Delta_\ell = \tau_\ell \varepsilon$, $\ell = 1, 2$, where $\varepsilon > 0$ and τ_1, τ_2 are relatively coprime integers satisfying $2 \leq \tau_1 < \tau_2$. For an input signal $g(t)$ with $\|g(t)\|_\infty \leq \frac{\tau_1 \tau_2 \varepsilon}{2}$ sampled at period T , let $y_\ell[k] = \langle g(kT) \rangle_{\Delta_\ell}$ denote the clean modulo samples, $\tilde{y}_1[k] = y_1[k] + e_1[k]$ the noisy samples at channel 1, and*

$$\tilde{s}[k] = \varepsilon d[k]/2 + e_s[k]$$

the sampled difference signal, where $d[k] = (y_2[k] - y_1[k])/\varepsilon$ is the normalised difference. Assume that $\tilde{y}_1[k]$ and $\tilde{s}[k]$ are quantised with $b \geq 1$ and b_d bits, respectively as in Alg. 1, giving a total bit cost

$$B_{\text{ECRT}} = b + b_d, \quad b_d = \lceil \log_2(\tau_1 + \tau_2) \rceil. \quad (12)$$

If the difference-path noise satisfies $|e_s[k]| < \varepsilon/4$, then the reconstruction error satisfies

$$|\hat{g}_{\text{ECRT}}[k] - g[k]| \leq \|e_1\|_\infty + \frac{\Delta_1}{2^{b+1}}, \quad (13)$$

where $\|e_1\|_\infty = \max_k |e_1[k]|$.

Proof: From the quantisation of $\tilde{s}[k]$ with step $\varepsilon/2$, the dequantised value satisfies $\hat{s}[k] = \tilde{s}[k] + q_s[k]$ with $|q_s[k]| \leq \varepsilon/4$. Under the noise condition $|e_s[k]| < \varepsilon/4$, we have

$$|\hat{s}[k] - \frac{\varepsilon d[k]}{2}| \leq |e_s[k]| + |q_s[k]| < \frac{\varepsilon}{2},$$

which ensures $\hat{d}[k] = \text{round}(2\hat{s}[k]/\varepsilon) = d[k]$. Hence the folding index of channel 1 is recovered exactly as $\hat{n}_1[k] = (\hat{d}[k]\gamma_1) \bmod \tau_2 = n_1[k]$, where γ_1 denotes the multiplicative inverse of τ_1 modulo τ_2 , i.e., $\gamma_1\tau_1 \equiv 1 \pmod{\tau_2}$.

The reconstructed signal can be expressed as

$$\hat{g}[k] = \hat{n}_1[k] \Delta_1 + \hat{y}_1[k] = n_1[k] \Delta_1 + (y_1[k] + e_1[k] + q_1[k]),$$

where $|q_1[k]| \leq \Delta_1/2^{b+1}$ is the channel-1 quantisation error. As $g[k] = n_1[k] \Delta_1 + y_1[k]$, we obtain

$$|\hat{g}[k] - g[k]| \leq |e_1[k]| + |q_1[k]| \leq \|e_1\|_\infty + \frac{\Delta_1}{2^{b+1}},$$

which proves (13). The bit cost (12) follows from Alg. 1. ■

B. Comparison with other schemes

Comparison with RCRT [18]. ECRT requires a fixed b_d bits to quantise $\tilde{s}(t)$, and channel 1 may use as little as $b = 1$ bit. In contrast, RCRT requires b to satisfy (12). Under this condition, combining (8) and (12) gives $B_{\text{RCRT}} - B_{\text{ECRT}} \geq 0$, showing that ECRT always achieves a smaller bit budget. In practice, forming the scaled difference $\tilde{s}[t]$ incurs negligible

Algorithm 1 ECRT Scheme**Require:** Noisy modulo output $\tilde{y}_1[k]$; difference signal $\tilde{s}[k]$;ADC parameters $\Delta_\ell, \tau_\ell, \varepsilon$ ($\ell = 1, 2$); bit budget b **Ensure:** Reconstructed sample $\hat{g}[k]$ **Transmitter:**1: Quantize $\tilde{y}_1(t)$ with step $\Delta_1/2^b$ (using b bits)2: $b_d = \lceil \log_2(\tau_1 + \tau_2) \rceil$ 3: Quantize $\tilde{s}(t)$ with step $\varepsilon/2$ (using b_d bits)**Receiver:**4: Dequantize to obtain $\hat{y}_1[k]$ and $\hat{s}[k]$ 5: $\hat{d}[k] = \text{round}(2\hat{s}[k]/\varepsilon)$ 6: $\hat{n}_1[k] = (\hat{d}[k]\gamma_1) \bmod \tau_2$, where $\gamma_1\tau_1 \equiv 1 \pmod{\tau_2}$ 7: $\hat{g}[k] = \hat{n}_1[k]\Delta_1 + \hat{y}_1[k]$

analog cost, as subtraction and scaling of $1/2$ are readily implemented by a simple operational amplifier. The noise term $e_s[k]$ is dominated by the modulo-stage errors, and the ECRT condition $|e_s[k]| < \varepsilon/4$ is effectively equivalent to the RCRT requirement $|e_2[k] - e_1[k]| < \varepsilon/2$, indicating that both schemes exhibit comparable noise tolerance.

For reconstruction error, when $\hat{n}_\ell[k] = n_\ell[k]$ for $\ell = 1, 2$, RCRT's averaging gives

$$\hat{g}_{\text{RCRT}}[k] - g[k] = \frac{1}{2}[(e_1[k] + q_1[k]) + (e_2[k] + q_2[k])].$$

With $\|e\|_\infty \triangleq \max_{k,\ell} |e_\ell[k]|$, this yields

$$|\hat{g}_{\text{RCRT}}[k] - g[k]| \leq \|e\|_\infty + \frac{\Delta_1 + \Delta_2}{2^{b+2}}.$$

Compared with (13), both schemes achieve the same worst-case error order. For average-case performance, the key distinction lies in how channel outputs are combined. ECRT reconstructs solely from the first-channel residue $\hat{y}_1[k] = y_1[k] + e_1[k] + q_1[k]$, yielding the error $e_1[k] + q_1[k]$. In contrast, RCRT averages both residues, and the reconstruction error is

$$\hat{g}_{\text{RCRT}}[k] - g[k] = \frac{1}{2}(e_1[k] + q_1[k] + e_2[k] + q_2[k]).$$

Under independent zero-mean noise,

$$\text{Var}(\hat{g}_{\text{RCRT}}[k] - g[k]) = \frac{1}{4}(\text{Var}(e_1 + q_1) + \text{Var}(e_2 + q_2))$$

which reduces to around $\frac{1}{2}\text{Var}(e_1 + q_1)$ when $\Delta_1 \approx \Delta_2$. Thus, RCRT nearly halves noise variance through averaging, while ECRT trades this reduction for lower bitrate.

Comparison with conventional ADC. We compare the ECRT against a conventional high-resolution ADC without saturation. For ECRT, the moduli $\tau_1 = \lceil \rho \rceil$, $\tau_2 = \lceil \rho \rceil + 1$ are chosen to maximize the error tolerance parameter ε for a given ρ [18], where $\lceil \cdot \rceil$ denotes the ceil operation.

Corollary 1. Let $\rho > 1$ be defined in (9). With B_c from (10) and B_{ECRT} from (12) using $\tau_1 = \lceil \rho \rceil$, $\tau_2 = \lceil \rho \rceil + 1$, for any integer $n \geq 1$,

$$B_{\text{ECRT}} = \begin{cases} B_c + 1, & 2^{n-1} < \rho \leq 2^n - 1, \\ B_c + 2, & 2^n - 1 < \rho \leq 2^n. \end{cases}$$

Proof: If $2^{n-1} < \rho \leq 2^n$, then $\lceil \log_2 \rho \rceil = n$ so $B_c = b + n$. For $2^{n-1} < \rho \leq 2^n - 1$, one has $2^{n-1} + 1 \leq \lceil \rho \rceil \leq 2^n - 1$, hence $2^n + 3 < 2\lceil \rho \rceil + 1 \leq 2^{n+1} - 1$, giving $\lceil \log_2(2\lceil \rho \rceil + 1) \rceil = n + 1$ and $B_{\text{ECRT}} = B_c + 1$. If $2^n - 1 < \rho \leq 2^n$, then $\lceil \rho \rceil = 2^n$ and $2^{n+1} < 2\lceil \rho \rceil + 1 \leq 2^{n+1} + 1$, yielding $\lceil \log_2(2\lceil \rho \rceil + 1) \rceil = n + 2$ and $B_{\text{ECRT}} = B_c + 2$. ■

TABLE I
THEORETICAL BITRATES (BPS) OF CONVENTIONAL ADC, SOSI [29] AND ECRT FOR SIGNAL BANDWIDTH 0.5 Hz (NYQUIST RATE 1 Hz).

b	ρ	R_c	R_{SOSI}	R_{ECRT}
3	5	6	28	7
	8	6	40	8
	10	7	48	8
6	5	9	49	10
	8	9	70	11
	10	10	84	11

1) $= n + 1$ and $B_{\text{ECRT}} = B_c + 1$. If $2^n - 1 < \rho \leq 2^n$, then $\lceil \rho \rceil = 2^n$ and $2^{n+1} < 2\lceil \rho \rceil + 1 \leq 2^{n+1} + 1$, yielding $\lceil \log_2(2\lceil \rho \rceil + 1) \rceil = n + 2$ and $B_{\text{ECRT}} = B_c + 2$. ■

Remark. A two-bit overhead arises only on the short interval $(2^n - 1, 2^n]$ (length 1) inside the dyadic range $(2^{n-1}, 2^n]$ (length 2^{n-1}). Hence, ECRT typically requires only one extra bit per signal sample compared with a conventional ADC, even though it operates with a much smaller dynamic range.

Comparison with single-channel systems. For a bandlimited signal $g(t)$ with finite energy, we benchmark the proposed design against single-channel modulo sampling with one-bit side information (SOSI) [29], [30], which provides closed-form guarantees on oversampling factor $\text{OF} \triangleq f_s/f_{\text{NYQ}}$ and stable recovery. From [29, Lem. 1 & Thm. 1], SOSI requires $b > 3$, $\text{OF} > 3$, and dynamic range $\rho \leq \text{OF} - 2$, yielding bit rate

$$R_{\text{SOSI}} = (b + 1) \text{OF} f_{\text{NYQ}} \geq (b + 1)(\rho + 2) f_{\text{NYQ}},$$

which scales *linearly* with ρ and incurs $\mathcal{O}(N^3)$ reconstruction complexity for N signal samples. In contrast, ECRT operates at Nyquist rate ($\text{OF} = 1$) with $\mathcal{O}(N)$ complexity and bit rate

$$R_{\text{ECRT}} = (b + \lceil \log_2(2\rho + 1) \rceil) f_{\text{NYQ}},$$

where $b = \Theta(\log \rho)$, yielding only *logarithmic* scaling in ρ . This makes ECRT substantially more efficient in bitrate-constrained scenarios, achieving comparable error to conventional ADCs without oversampling or complex decoding.

While these architectures represent different design trade-offs (oversampling versus multi-channel redundancy), ECRT is particularly advantageous for bandwidth-limited applications.

Remark. Under high oversampling, SOSI attains an MSE scaling of $\mathcal{O}(\text{OF}^{-3})$ [29, Thm. 1], surpassing the $\mathcal{O}(\text{OF}^{-1})$ decay of conventional oversampled ADCs, but only when $\text{OF} > \rho + 2$ and at the cost of increased bitrate and decoder complexity. Hardware results (Section IV) show that although SOSI offers slightly better accuracy at large oversampling factors, ECRT achieves comparable performance at substantially lower bitrate, making it preferable when communication bandwidth or receiver resources are constrained.

Sub-Nyquist Extension: For spectrally sparse signals, the proposed framework can be combined with multicoset sampling [31], [32] or coprime sensing [33], [34] to further reduce sampling rate. For example, introducing a delayed coset for each modulo channel (four branches total) [10]

TABLE II
BITRATE (KBPS) AND RRSE FOR A BANDLIMITED INPUT WITH $\rho = 2.8$ AND $B = 10$ kHz UNDER DIFFERENT QUANTISATION SCHEMES.

b	US-ALG [1]		USLSE [35]		SOSI [29]		Proposed ECRT	
	$f_s = 73.53$ kHz		$f_s = 119.05$ kHz		$b_e = 1$, $f_s = 51.02$ kHz	$b_d = 3$, $f_s = 20$ kHz		
	Bitrate	RRSE	Bitrate	RRSE	Bitrate	RRSE	Bitrate	RRSE
3	220.59	15.47	357.14	9.17×10^{-2}	204.08	7.21×10^{-2}	120.00	7.23×10^{-2}
4	294.12	4.52×10^{-2}	476.19	7.22×10^{-2}	255.10	4.95×10^{-2}	140.00	5.37×10^{-2}
5	367.65	3.62×10^{-2}	595.24	6.53×10^{-2}	306.12	3.99×10^{-2}	160.00	4.93×10^{-2}
6	441.18	3.17×10^{-2}	714.29	6.22×10^{-2}	357.14	3.87×10^{-2}	180.00	4.81×10^{-2}

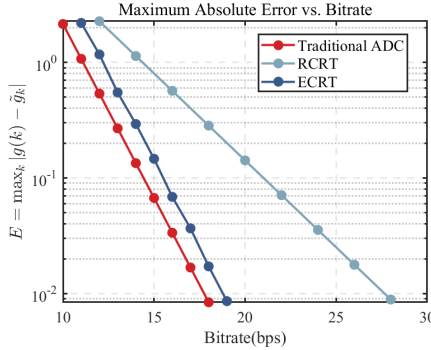


Fig. 2. MAE vs. transmission bitrate for conventional ADC, RCRT, and the proposed ECRT.

enables sampling periods $T > 1/f_{\text{NYQ}}$ while preserving sub-Nyquist spectral estimation. In this setting, ECRT performs quantisation and amplitude unfolding across each coset pair, providing bitrate-efficient amplitude unfolding. We leave this extension to future work.

IV. SIMULATION AND HARDWARE RESULTS

Simulation. We compare ECRT with conventional ADC and RCRT-based system [18] for a bandlimited input of bandwidth 0.5 Hz ($f_{\text{NYQ}} = 1$ Hz) and peak amplitude $\|g(t)\|_\infty = 22000$. With $\Delta_2 = 300$, the amplitude scaling factor is $\rho = 2\|g(t)\|_\infty/\Delta_2 = 14.67$. Following [18], the optimal two-channel setting uses consecutive coprimes $\tau_1 = \lceil \rho \rceil = 15$ and $\tau_2 = 16$, giving $\varepsilon = \Delta_2/\tau_2 \approx 18.75$ and thresholds $\Delta_1 \approx 281.25$, $\Delta_2 = 300$. Performance is measured by the maximum absolute error (MAE)

$$E = \max_k |g[k] - \hat{g}[k]|.$$

Fig. 2 shows MAE versus bitrate. As expected, the conventional ADC provides the benchmark, while ECRT closely follows with only a minor offset. In contrast, RCRT incurs higher redundancy since both channels are transmitted. For example, to achieve $MAE \approx 10^{-2}$, conventional ADC requires about 18 bps, ECRT 19 bps, whereas RCRT needs nearly 28 bps. These results are consistent with Corollary 1, confirming that ECRT introduces only a one-bit overhead per sample compared with a conventional ADC.

Hardware Experiment. We validate the proposed ECRT-based two-channel modulo ADC through experimental measurements obtained from our hardware prototype [36]. The setup uses $\Delta_1 = 0.72$ V and $\Delta_2 = 0.96$ V (i.e., $\tau_1 = 3$,

$\tau_2 = 4$ and $\varepsilon = 0.24$) to acquire a 10 kHz bandlimited signal ($\rho = 2.8$). Although our FPGA prototype supports real-time recovery using its on-board ADC [36], all hardware analog measurements in this section are acquired using an 8-bit Tektronix TDS 1012C-EDU oscilloscope. This ensures a fair comparison with single-channel systems: the oscilloscope is used to capture the ground-truth signal, the analog modulo outputs, and the analog difference signal, thereby avoiding additional scaling or timing jitter introduced by the on-board ADC. The reconstruction accuracy is then evaluated using the relative root-squared error (RRSE), defined as

$$\text{RRSE} = \sqrt{\frac{\sum_k |g[k] - \hat{g}[k]|^2}{\sum_k |g[k]|^2}}.$$

Table II compares the proposed ECRT with representative single-channel methods: US-ALG [1], USLSE [35], and SOSI [29]. ECRT quantises the scaled difference index with $b_d = 3$ bits, while SOSI uses one extra bit ($b_e = 1$). The results show that ECRT achieves comparable RRSE to the single-channel schemes, which require $f_s > 50$ kHz for similar fidelity, while operating at only 20 kHz. Across bit depths $b = 3\text{--}6$, ECRT achieves substantial bitrate reduction relative to SOSI, with negligible accuracy loss.

The theoretical analysis (Table I) predicts that ECRT's bitrate savings grow with ρ due to logarithmic scaling in bitrate. These experiments demonstrate substantial savings even at modest $\rho = 2.8$.

Remark. This comparison provides context rather than a strict benchmark, as single- and multi-channel architectures embody different tradeoffs: single-channel schemes rely on oversampling and complex recovery for hardware compactness, whereas ECRT leverages channel diversity for Nyquist-rate sampling with $\mathcal{O}(N)$ CRT-based reconstruction at the cost of additional front-end circuitry.

V. CONCLUSION

This paper presented an ECRT scheme for two-channel modulo ADCs that transmits one quantised channel together with a scaled difference, thereby removing the redundancy of RCRT while preserving robustness to folding and quantisation errors. The analysis shows that the required bitrate grows only logarithmically with ρ , and hardware results demonstrate comparable robustness at substantially lower bitrates. These features make ECRT well suited for low-bitrate, high-fidelity acquisition in resource-limited sensing systems.

REFERENCES

- [1] A. Bhandari, F. Krahmer, and R. Raskar, "On unlimited sampling and reconstruction," *IEEE Trans. Signal Process.*, vol. 69, pp. 3827–3839, 2021.
- [2] A. Bhandari, F. Krahmer, and T. Poskitt, "Unlimited sampling from theory to practice: Fourier–Prony recovery and prototype ADC," *IEEE Trans. Signal Process.*, vol. 70, pp. 1131–1141, 2022.
- [3] A. Bhandari, F. Krahmer, and R. Raskar, "Unlimited sampling of sparse signals," in *Proc. IEEE Int. Conf. Acoust., Speech Signal Process. (ICASSP)*, 2018, pp. 4569–4573.
- [4] G. Shtendel, D. Florescu, and A. Bhandari, "Unlimited sampling of bandpass signals: computational demodulation via undersampling," *IEEE Trans. Signal Process.*, vol. 71, pp. 4134–4145, 2023.
- [5] A. Bhandari, "Back in the US-SR: unlimited sampling and sparse super-resolution with its hardware validation," *IEEE Signal Process. Lett.*, vol. 29, pp. 1047–1051, 2022.
- [6] D. Florescu, F. Krahmer, and A. Bhandari, "The surprising benefits of hysteresis in unlimited sampling: theory, algorithms and experiments," *IEEE Trans. Signal Process.*, vol. 70, pp. 616–630, 2022.
- [7] D. Florescu and A. Bhandari, "Time encoding via unlimited sampling: theory, algorithms and hardware validation," *IEEE Trans. Signal Process.*, vol. 70, pp. 4912–4924, 2022.
- [8] G. Shtendel and A. Bhandari, "HDR-TOF: HDR time-of-flight imaging via modulo acquisition," in *Proc. IEEE Int. Conf. Image Process. (ICIP)*, 2022, pp. 3808–3812.
- [9] R. Guo and A. Bhandari, "ITER-SIS: robust unlimited sampling via iterative signal sieving," in *Proc. IEEE Int. Conf. Acoust., Speech Signal Process. (ICASSP)*, 2023, pp. 1–5.
- [10] R. Guo, Y. Zhu, and A. Bhandari, "Sub-Nyquist USF spectral estimation: K frequencies with $6K + 4$ modulo samples," *IEEE Trans. Signal Process.*, vol. 72, pp. 5065–5076, 2024.
- [11] H. Wang, J. Fang, H. Li, G. Leus, R. Zhu, and L. Gan, "Line spectral estimation with unlimited sensing," *Signal Processing*, p. 110205, 2025.
- [12] T. Feuillen, B. S. MRR, and A. Bhandari, "Unlimited sampling radar: life below the quantization noise," in *Proc. IEEE Int. Conf. Acoust., Speech Signal Process. (ICASSP)*, 2023, pp. 1–5.
- [13] S. Mulleti, E. Reznitskiy, S. Savariego, M. Namer, N. Glazer, and Y. C. Eldar, "A hardware prototype of wideband high-dynamic range analog-to-digital converter," *IET Circuits, Devices & Systems*, vol. 17, no. 4, pp. 181–192, 2023.
- [14] Y. Zhu, R. Guo, and A. Bhandari, "Ironing the modulo folds: unlimited sensing with $100 \times$ bandwidth expansion," in *Proc. 15th Int. Conf. Sampling Theory Appl. (SampTA)*, 2025.
- [15] J. Zhu, J. Ma, Z. Liu, F. Qu, Z. Zhu, and Q. Zhang, "A modulo sampling hardware prototype and reconstruction algorithms evaluation," *IEEE Trans. Instrum. Meas.*, vol. 74, pp. 1–11, 2025.
- [16] L. Gan and H. Liu, "High dynamic range sensing using multi-channel modulo samplers," in *Proc. IEEE 11th Sensor Array Multichannel Signal Process. Workshop (SAM)*, 2020, pp. 1–5.
- [17] Y. Gong, L. Gan, and H. Liu, "Multi-channel modulo samplers constructed from Gaussian integers," *IEEE Signal Process. Lett.*, vol. 28, pp. 1828–1832, 2021.
- [18] W. Yan, L. Gan, S. Hu, and H. Liu, "Towards optimized multi-channel modulo-ADCs: moduli selection strategies and bit depth analysis," in *Proc. IEEE Int. Conf. Acoust., Speech Signal Process. (ICASSP)*, 2024, pp. 9496–9500.
- [19] W. Yan, L. Gan, and Y. D. Zhang, "Threshold sensitivity in two-channel modulo-ADCs: analysis and robust reconstruction," in *Proc. IEEE Int. Conf. Acoust., Speech Signal Process. (ICASSP)*, 2025, pp. 1–5.
- [20] W. Yan, R. Zhu, Z. Li, L. Gan, and H. Liu, "Parameter selection in complex-valued two-channel modulo-ADC sampling system," in *Proc. Int. Conf. Sampling Theory Appl. (SampTA)*, 2025, pp. 1–5.
- [21] W. Wang and X.-G. Xia, "A closed-form robust Chinese remainder theorem and its performance analysis," *IEEE Trans. Signal Process.*, vol. 58, no. 11, pp. 5655–5666, 2010.
- [22] L. Xiao and X.-G. Xia, "A generalized Chinese remainder theorem for two integers," *IEEE Signal Process. Lett.*, vol. 21, no. 1, pp. 55–59, 2014.
- [23] L. Xiao and X.-G. Xia, "Error correction in polynomial remainder codes with non-pairwise coprime moduli and robust Chinese remainder theorem for polynomials," *IEEE Trans. Commun.*, vol. 63, no. 3, pp. 605–616, 2015.
- [24] R. Guo and A. Bhandari, "Unlimited sampling of FRI signals independent of sampling rate," in *Proc. IEEE Int. Conf. Acoust., Speech Signal Process. (ICASSP)*, 2023, pp. 1–5.
- [25] Y. Zhu, R. Guo, P. Zhang, and A. Bhandari, "Frequency estimation via sub-Nyquist unlimited sampling," in *Proc. IEEE Int. Conf. Acoust., Speech Signal Process. (ICASSP)*, 2024, pp. 9636–9640.
- [26] V. Pavlíček, R. Guo, and A. Bhandari, "Bits, channels, frequencies and unlimited sensing: pushing the limits of sub-Nyquist Prony," in *Proc. Eur. Signal Process. Conf. (EUSIPCO)*, 2024, pp. 2462–2466.
- [27] H. Wang, J. Fang, X. Zheng, H. Li, and J. Wang, "Estimating a mixture of sinusoids with multi-channel unlimited sampling," in *Proc. Eur. Signal Process. Conf. (EUSIPCO)*, 2025.
- [28] D. Florescu, "Multichannel modulo sampling with unlimited noise," in *Proc. IEEE Int. Conf. Acoust., Speech Signal Process. (ICASSP)*, 2025, pp. 1–5.
- [29] N. I. Bernardo, S. B. Shah, and Y. C. Eldar, "Modulo sampling with 1-bit side information: performance guarantees in the presence of quantization," in *Proc. IEEE Int. Symp. Inf. Theory (ISIT)*, 2024, pp. 3498–3503.
- [30] N. I. Bernardo, S. B. Shah, and Y. C. Eldar, "Modulo sampling: performance guarantees in the presence of quantization," *IEEE Trans. Signal Process.*, vol. 73, pp. 3829–3842, 2025.
- [31] J. Zhang, P. Liu, N. Fu, and X. Peng, "Prototype design of multicoset sampling based on compressed sensing," in *Proc. IEEE Int. Conf. Electron. Meas. Instrum. (ICEMI)*, 2015, pp. 1303–1308.
- [32] D. D. Ariananda, G. Leus, and Z. Tian, "Multi-coset sampling for power spectrum blind sensing," in *Proc. Int. Conf. Digit. Signal Process. (DSP)*, 2011, pp. 1–8.
- [33] L. Xiao, X.-G. Xia, and W. Wang, "Multi-stage robust Chinese remainder theorem," *IEEE Trans. Signal Process.*, vol. 62, no. 18, pp. 4772–4785, 2014.
- [34] H. Liang, X. Li, and X.-G. Xia, "Adaptive frequency estimation with low sampling rates based on robust Chinese remainder theorem and IIR notch filter," in *Proc. IEEE Conf. Ind. Electron. Appl. (ICIEA)*, 2009, pp. 2999–3004.
- [35] Q. Zhang, J. Zhu, F. Qu, and D. W. Soh, "Line spectral estimation via unlimited sampling," *IEEE Trans. Aerosp. Electron. Syst.*, vol. 60, no. 5, pp. 7214–7231, 2024.
- [36] Z. Li, W. Yan, R. Zhu, L. Gan, and H. Liu, "Live demonstration: real-time high-amplitude signal acquisition with 2-channel modulo ADC," in *Proc. IEEE Int. Symp. Circuits Syst. (ISCAS)*, 2025, pp. 1–1.